ICINCO 2023

20th International Conference on Informatics in Control, Automation and Robotics

PROCEEDINGS

Volume 1

13 - 15 November, 2023

EDITORS

Giuseppina Gini
Henk Nijmeijer
Dimitar Filev

https://icinco.scitevents.org

SPONSORED BY
INSTICC

PAPERS AVAILABLE AT
SCITEPRESS DIGITAL LIBRARY

ICINCO 2023

Proceedings of the
20th International Conference on
Informatics in Control, Automation and Robotics

Volume 1

Rome - Italy

November 13 - 15, 2023

Sponsored by
INSTICC - Institute for Systems and Technologies of Information, Control and Communication

Technically Co-sponsored by
IFAC - International Federation of Automatic Control

ACM In Cooperation
SIGAI - ACM Special Interest Group on Artificial Intelligence

In Cooperation with
AAAI - Association for the Advancement of Artificial Intelligence
INNS - International Neural Network Society

Copyright © 2023 by SCITEPRESS – Science and Technology Publications, Lda.
Under CC license (CC BY-NC-ND 4.0)

Edited by Giuseppina Gini, Henk Nijmeijer and Dimitar Filev

Printed in Portugal
ISSN: 2184-2809
ISBN: 978-989-758-670-5
DOI: 10.5220/0000168300003543
Depósito Legal: 519637/23

https://icinco.scitevents.org
icinco.secretariat@insticc.org

BRIEF CONTENTS

INVITED SPEAKERS IV

ORGANIZING COMMITTEES V

PROGRAM COMMITTEE VI

AUXILIARY REVIEWERS IX

SELECTED PAPERS BOOK IX

FOREWORD XI

CONTENTS XIII

INVITED SPEAKERS

Luís Paulo Reis
University of Porto
Portugal

Wim Michiels
KU Leuven
Belgium

Anuradha Annaswamy
MIT
United States

Sergio M. Savaresi
Politecnico di Milano
Italy

ORGANIZING COMMITTEES

CONFERENCE CHAIR

Dimitar Filev, Research & Advanced Engineering, Ford Motor Company, United States

PROGRAM CO-CHAIRS

Giuseppina Gini, Politecnico di Milano, Italy
Henk Nijmeijer, Eindhoven University of Technology, Netherlands

LOCAL CHAIRS

Paolo Di Giamberardino, Sapienza University of Rome, Italy
Daniela Iacoviello, Sapienza University of Rome, Italy

SECRETARIAT

Ana Rita Paciência, INSTICC, Portugal

GRAPHICS PRODUCTION AND WEBDESIGNER

André Fernandes, INSTICC, Portugal
Inês Teles, INSTICC, Portugal

WEBMASTER

João Francisco, INSTICC, Portugal
Carolina Ribeiro, INSTICC, Portugal

PROGRAM COMMITTEE

Hussein Abdullah, University of Guelph, Canada

El-Houssaine Aghezzaf, Ghent University, Faculty of Engineering and Architecture, Belgium

Eugenio Aguirre, University of Granada, Spain

Rudy Agustriyanto, University of Surabaya, Indonesia

Mojtaba Ahmadieh Khanesar, University of Nottingham, United Kingdom

Carlos Aldana, University of Guadalajara, Mexico

Manuel Aleixandre, Tokyo Institute of Technology, Japan

Joaquin Alvarez, Center Scientific Research Higher Education Ensenada Cicese, Mexico

Mihail Antchev, Technical University - Sofia, Bulgaria

Rui Araujo, University of Coimbra, Portugal

Mohd Ashraf Ahmad, University Malaysia Pahang, Malaysia

Ramiro Barbosa, ISEP/IPP - School of Engineering, Polytechnic Institute of Porto, Portugal

Michele Basso, University of Florence, Italy

Eric Baumgartner, Milwaukee School of Engineering, United States

Mahmoud Belhocine, CDTA, Algeria

Juri Belikov, Tallinn University of Technology, Estonia

Karsten Berns, University of Kaiserslautern-Landau, Germany

Sylvain Bertrand, ONERA - Univ. Paris-Saclay, France

Zafer Bingul, Kocaeli University, Turkey

Claudia-Adina Bojan-Dragos, Politehnica University of Timisoara, Romania

Magnus Boman, The Royal Institute of Technology, Sweden

Mohammad Bozorg, Yazd University, Iran, Islamic Republic of

Richard Braatz, Massachusetts Institute of Technology, United States

Laurent Burlion, Rutgers, the State University of New Jersey, United States

Simeon C. Calvert, TU Delft, Netherlands

Kenneth Camilleri, University of Malta, Malta

Enrique Carrera, Army Polytechnic School Ecuador, Ecuador

Marco Castellani, University of Birmingham, United Kingdom

Paul Christodoulides, Cyprus University of Technology, Cyprus

Feng Chu, University of Evry Val d'Essonne, France

Marco Costanzo, Università degli Studi della Campania Luigi Vanvitelli, Italy

Michel Dambrine, Polytechnic University of Hauts-de-France, France

Paolo Di Giamberardino, Sapienza University of Rome, Italy

António Dourado, University of Coimbra, Portugal

Marc Ebner, Ernst-Moritz-Arndt-Universität Greifswald, Germany

Mehmet Önder Efe, Hacettepe Univ., Turkey

Ali Eydgahi, Eastern Michigan University, United States

Mohammed Fadali, UNR, United States

Baris Fidan, University of Waterloo, Canada

Paolo Fiorini, University of Verona, Italy

Thierry Fraichard, INRIA, France

Giuseppe Franze', University of Calabria, Italy

Eduardo Oliveira Freire, Federal University of Sergipe, Brazil

Georg Frey, Automation and Energy Systems, Saarland University, Germany

Toyomi Fujita, Tohoku Institute of Technology, Japan

Andrej Gams, Jožef Stefan Institute, Slovenia

Péter Gáspár, SZTAKI, Hungary

Eduardo Godoy, São Paulo State University (UNESP), Brazil

Arthur Gómez, Universidade do Vale do Rio dos Sinos, Brazil

Juan-Jose Gonzalez De La Rosa, University of Cadiz, Spain

Corrado Guarino Lo Bianco, Università di Parma, Italy

Prof. Rajeev Gupta, Rajasthan Technical University, India

Kensuke Harada, Osaka University, Japan

Khalifa Harib, UAE University, United Arab Emirates

Hiroshi Hashimoto, Advanced Institute of Industrial Technology, Japan

Ramdane Hedjar, King Saud University, Saudi Arabia

Ghaleb Hoblos, Graduate School of Electrical Engineering, France

Wladyslaw Homenda, Warsaw University of Technology, Poland

Chiu-Fan Hsieh, National Formosa University, Taiwan, Republic of China

Liu Hsu, COPPE-UFRJ, Brazil

Daniela Iacoviello, Sapienza University of Rome, Italy

Junichi Iijima, Tokyo Institute of Technology, Japan

Gian Paolo Incremona, Politecnico di Milano, Italy

Gianluca Ippoliti, Università Politecnica delle Marche, Italy

Sarangapani Jagannathan, Missouri University of Science and Technology, United States

Isabel Jesus, ISEP/IPP - School of Engineering, Polytechnic Institute of Porto, Portugal

Fabrício Junqueira, University of São Paulo (USP), Brazil

Tohru Kawabe, University of Tsukuba, Japan

Balint Kiss, Budapest University of Technology and Economics, Hungary

Bahare Kiumarsi, Michigan State University, United States

Peter Košťál, Slovenská Technická Univerzita v Bratislave, Slovak Republic

Marek Kraft, Poznan University of Technology, Poland

Dragana Krstic, University of Nis, Faculty of Electronic Engineering, Serbia

Masao Kubo, Narional Defense Academy of Japan, Japan

Kolja Kühnlenz, Coburg University of Applied Sciences and Arts, Germany

Miroslav Kulich, Czech Technical University in Prague, Czech Republic

Sébastien Lahaye, Istia - LARIS, France

Ho-Hoon Lee, Southeastern Louisiana University, United States

Kauko Leiviskä, University of Oulu, Finland

Gordon Lightbody, University College Cork, Ireland

Antonio Lopes, University of Porto, Portugal

Anthony Maciejewski, Colorado State University, United States

Mohammad Javad Mahmoodabadi, Sirjan University of Technology, Iran, Islamic Republic of

Om Malik, University of Calgary, Canada

Federico Mari, University of Rome Foro Italico, Italy

Ester Martinez-Martin, University of Alicante, Spain

Jorge Martins, Instituto Superior Técnico, Portugal

Lorinc Marton, Sapientia Hungarian University of Transylvania, Romania

Pavlo Maruschak, Ternopil National Ivan Puluj Technical University, Ukraine

Luca Mazzola, HSLU - Lucerne University of Applied Sciences, Switzerland

Seán McLoone, Queen’s Unviersity Belfast, Ireland

Mahanijah Md Kamal, Universiti Teknologi MARA, Malaysia

Nadhir Messai, University of Reims Champagne-Ardenne, France

Maciej Michalek, Poznan University of Technology, Poland

Marek Miskowicz, AGH University of Science and Technology, Poland

Paulo Miyagi, University of Sao Paulo, Brazil

Héctor Montes, Technological University of Panama, Panama

Rafael Morales, University of Castilla La Mancha, Spain

Vidal Moreno Rodilla, Universidad De Salamanca, Spain

George Moustris, National Technical University of Athens, Greece

Riccardo Muradore, University of Verona, Italy

Naresh N. Nandola, Siemens Technology, United States

Ciro Natale, Università degli Studi della Campania Luigi Vanvitelli, Italy

Juan J. Nieto, University of Santiago de Compostela, Spain

Shimon Nof, Purdue University, United States

Urbano Nunes, University of Coimbra, Portugal

Andrzej Obuchowicz, University of Zielona Góra, Poland

Fernando Osorio, USP - Universidade de Sao Paulo, Brazil

Stamatios Papadakis, Department of Preschool Education, Faculty of Education, University of Crete, Greece

Evangelos Papadopoulos, NTUA, Greece

Ju H. Park, Yeungnam University, Korea, Republic of

Igor Paromtchik, Robotic Technologies, France

Dariusz Pazderski, Poznan University of Technology, Poland

Qingjin Peng, University of Manitoba, Canada

Tadej Petric, Jožef Stefan Institute, Slovenia

Mark Post, The University of York, United Kingdom

Raul Marin Prades, Jaume I University, Spain

Radu-Emil Precup, Politehnica University of Timisoara, Romania

Kanty Rabenorosoa, Femto-ST Institute, France

Navid Razmjooy, Independent Researcher, Iran, Islamic Republic of

Oscar Reinoso, Miguel Hernandez University, Spain

Gerasimos Rigatos, Industrial Systems Institute, Greece

Paolo Rocco, Politecnico di Milano, Italy

Alejandro Rodriguez-Angeles, Cinvestav-IPN, Mexico

Raul-Cristian Roman, Politehnica University of Timisoara, Romania

Juha Röning, University of Oulu, Finland

Christophe Sabourin, Univ. Paris Est Creteil, LISSI, France

Antonio Sala, Universitat Politecnica de Valencia, Spain

Addisson Salazar, Universitat Politècnica de València, Spain

Javier Sanchis, Universitat Politècnica de València, Spain

Jurek Sasiadek, Carleton University, Canada

Dieter Schramm, University of Duisburg-Essen, Germany

Karol Seweryn, Space Research Centre (CBK PAN), Poland

Antonio Sgorbissa, University of Genova, Italy

Madhavan Shanmugavel, SRM Institute of Science and Technology, India

Jinhua She, Tokyo University of Technology, Japan

Milad Siami, Massachusetts Institute of Technology, United States

Vasile Sima, Technical Sciences Academy of Romania, Romania

Azura Che Soh, Universiti Putra Malaysia, Malaysia

Paolo Stegagno, University of Rhode Island, United States

Adrian-Mihail Stoica, Polytechnic University Bucharest, Romania

Olaf Stursberg, University of Kassel, Germany

József Tar, Óbuda University, Hungary

Tomasz Tarczewski, Nicolaus Copernicus University, Poland

Daniel Thalmann, Ecole Polytechnique Federale de Lausanne, Switzerland

Gui Tian, Newcastle University, United Kingdom

Germano Torres, PS Solutions, Brazil

Andrés Úbeda, University of Alicante, Spain

José Valente de Oliveira, Universidade do Algarve, Portugal

Luigi Villani, Università di Napoli Federico II, Italy

Blas Vinagre, University of Extremadura, Spain

Antonio Visioli, University of Brescia, Italy

Damir Vrancic, Jožef Stefan Institute, Slovenia

Qiangda Yang, Northeastern University, China

Sho Yokota, Toyo University, Japan

Hongnian Yu, Bournemouth University, United Kingdom

Jie Zhang, Newcastle University, United Kingdom

Cezary Zielinski, Warsaw University of Technology, Poland

AUXILIARY REVIEWERS

Fabiano Correa, University of Sao Paulo, Brazil

Raul Cruz-Morales, UNAM-FES-Cuautitlan, Mexico

Luís Garrote, ISR-UC, Portugal

Vesna Javor, Independent Researcher, Serbia

Abdelhai Lati, University of Ouargla, Algeria

Balazs Nemeth, Institute for Computer Science and Control, Hungary

Pouya Panahandeh, University of Waterloo, Canada

João Paulo, Instituto de Sistemas e Robótica (ISR-UC), Portugal

Ricardo Pereira, Instituto de Sistemas e Robótica ISR-UC, Portugal

Nenad Petrovic, University of Nis, Faculty of Electronic Engineering, Serbia

Rafal Sobanski, Poznan University of Technology, Poland

Xinyue Wang, University of Paris-Saclay, France

SELECTED PAPERS BOOK

A number of selected papers presented at ICINCO 2023 will be published by Springer in a LNEE Series book. This selection will be done by the Conference Chair and Program Co-chairs, among the papers actually presented at the conference, based on a rigorous review by the ICINCO 2023 Program Committee members.

FOREWORD

This book contains the proceedings of the 20th International Conference on Informatics in Control, Automation and Robotics (ICINCO 2023), held in Rome, Italy from 13 – 15 November, 2023.

ICINCO is sponsored by the Institute for Systems and Technologies of Information, Control and Communication (INSTICC), technically co-sponsored by the International Federation of Automatic Control (IFAC) and held in cooperation with the ACM Special Interest Group on Artificial Intelligence, Association for the Advancement of Artificial Intelligence (AAAI) and the International Neural Network Society (INNS).

The ICINCO conference series has now become a major forum to debate technical and scientific advances presented by researchers and developers both from academia and industry, working in areas related to Control, Automation and Robotics that benefit from Information Technology.

The high quality of the ICINCO 2023 program is enhanced by four keynote lectures, given by internationally recognized researchers, namely: Luís Paulo Reis (University of Porto, Portugal), Wim Michiels (KU Leuven, Belgium), Anuradha Annaswamy (MIT, United States), and Sergio M. Savaresi (Politecnico di Milano, Italy).

ICINCO 2023 received 180 paper submissions from 47 countries of which 20% were accepted as full papers. To evaluate each submission, a double-blind paper review process was performed and lead by the Program Committee. As in previous editions of the conference, based on the reviewer's evaluations and the presentations, selected authors with the best papers will be invited to submit extended versions for a special issue in the Springer Nature Computer Science Journal, and a book in the Springer Lecture Notes in Electrical Engineering series.

We would like to express our thanks and appreciations to all participants. First, to the authors, whose quality work is the essence of this conference. Second, to all the members of the Program Committee and all reviewers, who helped with their expertise and valuable time they have invested in reviewing submitted papers. We would also like to deeply thank the invited speakers for their excellent contributions and sharing their knowledge and vision. Finally, a word of appreciation for the hard work of the INSTICC team; organizing a conference of this level is a task that can only be achieved by the collaborative effort of a dedicated and highly capable team.

We hope that you will enjoy the conference, the discussions with other participants, and the nice Italian atmosphere.

Finally, we look forward to have additional research results presented at the next edition of ICINCO.

Giuseppina Gini
Politecnico di Milano, Italy

Henk Nijmeijer
Eindhoven University of Technology, Netherlands

Dimitar Filev
Research & Advanced Engineering, Ford Motor Company, United States

CONTENTS

INVITED SPEAKERS

KEYNOTE SPEAKERS

Deep Reinforcement Learning for Creating Advanced Humanoid Robotic Soccer Skills
Luís Paulo Reis 5

Analysis and Control Design Tools for Dynamical Systems with Time-Delay
Wim Michiels 7

Lessons from Adaptive Control: Towards Real-Time Machine Learning
Anuradha Annaswamy 9

Autonomous Driving: The Hidden Enabling Technology for a Sustainable Mobility Model
Sergio M. Savaresi 11

INTELLIGENT CONTROL SYSTEMS AND OPTIMIZATION

FULL PAPERS

A Dynamic Computational Model of Head Sway Responses in Human Upright Stance Postural Control During Support Surface Tilt 17
Vittorio Lippi, Christoph Maurer and Stefan Kammermeier

Locally Convex Neural Lyapunov Functions and Region of Attraction Maximization for Stability of Nonlinear Systems 29
Lucas Hugo, Philippe Feyel and David Saussié

Nonlinear Model Predictive Control for Uranium Extraction-Scrubbing Operation in Spent Nuclear Fuel Treatment Process 37
Duc-Tri Vo, Ionela Prodan, Laurent Lefèvre, Vincent Vanel, Sylvain Costenoble and Binh Dinh

Positively Invariant Sets for ODEs and Numerical Integration
Peter Giesl, Sigurdur Hafstein and Iman Mehrabinezhad 44

Maritime Dynamic Resource Allocation and Risk Minimization Using Visual Analytics and Elitist Multi-Objective Optimization 54
Mayamin Hamid Raha, Md. Abu Sayed, Monica Nicolescu, Mircea Nicolescu and Sushil Louis

Stereo Video Camera Calibration in the Wild
Arhum Sultana and Michael Jenkin 64

Enhanced Optimal Beacon Placement for Indoor Positioning: A Set Variable Based Constraint Programming Approach 70
Sven Löffler, Ilja Becker, Carlo B. ückert and Petra Hofstedt

Neural-Network for Position Estimation of a Cable-Suspended Payload Using Inertial Quadrotor Sensing 80
Julien Mellet, Jonathan Cacace, Fabio Ruggiero and Vincenzo Lippiello

Variable Trust Setting for Safe and Ethical Algorithms for Navigation of Autonomous Vehicles (C-NAV) on a Highway 88
Joshua D'Souza, Jisun Kim and James E. Pickering

Explainable Machine Learning for Evapotranspiration Prediction
Bamory Ahmed Toru Koné, Rima Grati, Bassem Bouaziz and Khouloud Boukadi 97

SHORT PAPERS

A Concept for Optimizing Motor Control Parameters Using Bayesian Optimization
Henning Cui, Markus Görlich-Bucher, Lukas Rosenbauer, Jörg Hähner and Daniel Gerber 107

Technological Solution for Crime Prevention in Los Olivos
Juan-Pablo Mansilla, Matías Beteta and David Castañeda 115

On Selecting Optimal Hyperparameters for Reinforcement Learning Based Robotics Applications: A Practical Approach
Ignacio Fidalgo, Guillermo Villate, Alberto Tellaeche and Juan Ignacio Vázquez 123

Fractional Order-Sliding-Mode Controller for Regulation of a Nonlinear Chemical Process with Variable Delay
Antonio Di Teodoro, Marco Herrera and Oscar Camacho 131

Experimental Investigation and Comparison of Approaches for Correcting Acceleration Phases in Motor Torque Signal of Electromechanical Axes
Chris Schöberlein, André Sewohl, Holger Schlegel and Martin Dix 140

Probabilistic Physics-Augmented Neural Networks for Robust Control Applied to a Slider-Crank System
Edward Kikken, Jeroen Willems, Rob Salaets and Erik Hostens 152

A Clustering-Based Approach for Adaptive Control Applied to a Hybrid Electric Vehicle
Rian Beck, Sudarsan Kumar Venkatesan, Joram Meskens, Jeroen Willems, Edward Kikken and Bruno Depraetere 162

Mapping, Localization and Navigation for an Assistive Mobile Robot in a Robot-Inclusive Space
Prabhu R. Naraharisetti, Michael A. Saliba and Simon G. Fabri 172

Data Digitalization and Conformity Verification in Oil and Gas Industry Databooks Using Semantic Model Based on Ontology
Mario Ricardo Nascimento Marques Junior, Eder Mateus Nunes Gonçalves, Silvia Silva da Costa Botelho and Emanuel da Silva Diaz Estrada 180

Kinematics Based Joint-Torque Estimation Using Bayesian Particle Filters
Roja Zakeri and Praveen Shankar 188

Contraction Metrics by Numerical Integration and Quadrature: Uniform Error Estimate
Peter Giesl, Sigurdur Hafstein and Iman Mehrabinezhad 196

Dynamic Periodic Event-Triggered Control for Linear Systems Based on Partial State Information
Mahmoud Abdelrahim and Dhafer Almakhles 206

An Unsupervised Neural Network Approach for Solving the Optimal Power Flow Problem
Alexander Svensson Marcial and Magnus Perninge 214

Multi-Agent Pathfinding for Indoor Quadcopters: A Platform for Testing Planning-Acting Loop
Matouš Kulhan and Pavel Surynek 221

Trajectory Planning for Multiple Vehicles Using Motion Primitives: A Moving Horizon Approach Under Uncertainty
Bahaaeldin Elsayed and Rolf Findeisen 229

Fault Diagnosis with Stacked Sparse AutoEncoder for Multimode Process Monitoring
Yahia Kourd, Messaoud Ramdani, Riadh Toumi and Ahmed Samet 237

Hand Gesture Interface to Teach an Industrial Robots
Mojtaba Ahmadieh Khanesar and David Branson 243

Emergency Meteorological Data Preparation for Artillery Operations
Jan Ivan, Michal Šustr, David Sládek, Jaroslav Varecha and Jiří Gregor 250

Spectral Clustering in Rule-Based Algorithms for Multi-Agent Path Finding
Irene Saccani, Kristýna Janovská and Pavel Surynek 258

Creating of Minefield Breaches with Artillery
Michal Švehlík, Michal Šustr, Ladislav Potužák, Jaroslav Varecha and Jan Drábek 266

CFRLI-IDM: A Counterfactual Risk Level Inference Based Intelligence Driver Model for Extremely Aggressive Cut-in Scenario in China
Yongqiang Li, Yang Lv, Quan Wang and Qiankun Miao 273

Mobile Robot Navigation Based on Pedestrian Flow Model Considering Human Unsteady Dynamic Behavior
Ryusei Shigemoto and Ryosuke Tasaki 281

A Study on Acquisition of 3D Self-Localization by Fluorescent Lights
Rikuto Ozawa and Hiroyuki Kobayashi 285

Decentralized Federated Learning Architecture for Networked Microgrids
Ilyes Naidji, Chams Eddine Choucha and Mohamed Ramdani 291

Distributed Predictive Control for Roundabout Crossing Modelled by Virtual Platooning
Alessandro Bozzi, Simone Graffione, Roberto Sacile and Enrico Zero 295

Interval Type-2 Fuzzy Control to Solve Containment Problem of Multiple USV with Leader's Formation Controller
Wen-Jer Chang, Yann-Horng Lin and Cheung-Chieh Ku 302

A Study on the Energy Efficiency of Various Gaits for Quadruped Robots: Generation and Evaluation
Roman Zashchitin and Dmitrii Dobriborsci 311

Offline Feature-Based Reinforcement Learning with Preprocessed Image Inputs for Liquid Pouring Control
Stephan Pareigis, Jesus Eduardo Hermosilla-Diaz, Jeeangh Jennessi Reyes-Montiel, Fynn Luca Maaß, Helen Haase, Maximilian Mang and Antonio Marin-Hernandez 320

Preliminary Results on Controllability of Serial Robot-Manipulators in Singular Configurations
Mir Mamunuzzaman and Jörg Mareczek 327

A Meta-Review on the Use of Artificial Intelligence in the Context of Electrical Power Grid Operators
Daniel Staegemann, Christian Haertel, Christian Daase, Matthias Pohl and Klaus Turowski 335

Proposal of a New Approach Using Deep Learning for QR Code Embedding
Kanaru Kumabuchi and Hiroyuki Kobayashi 342

Hand-Drawn Diagram Correction Using Machine Learning
Tenga Yoshida and Hiroyuki Kobayashi 346

University Recommendation System for Undergraduate Studies in Bangladesh Using Distributed Machine Learning
Ahmed Nur Merag, Rezwana Chaudhury Raka, Sumya Afroj, Md Humaion Kabir Mehedi and Annajiat Alim Rasel 352

ROBOTICS AND AUTOMATION

FULL PAPERS

Hanging Drone: An Approach to UAV Landing for Monitoring
Alan Kunz Cechinel, Juha Röning, Antti Tikanmaki, Edson Roberto DePieri and Patricia Della Méa Plentz 363

CASP: Computer Aided Specimen Placement for Robot-Based Component Testing
Julian Hanke, Matthias Stueben, Christian Eymüller, Maximilian Enrico Müller, Alexander Poeppel and Wolfgang Reif 374

Computing the Traversability of the Environment by Means of Sparse Convolutional 3D Neural Networks
Antonio Santo, Arturo Gil, David Valiente, Mónica Ballesta and Adrián Peidró 383

Experimental Validation of an Actor-Critic Model Predictive Force Controller for Robot-Environment Interaction Tasks
Alessandro Pozzi, Luca Puricelli, Vincenzo Petrone, Enrico Ferrentino, Pasquale Chiacchio, Francesco Braghin and Loris Roveda 394

Robot Path Planning with Safety Zones
Evis Plaku, Arben Çela and Erion Plaku 405

Comparative Analysis of Segmentation Techniques for Reticular Structures
Francisco J. Soler, Luis M. Jiménez, David Valiente, Luis Payá and Óscar Reinoso 413

Learning-Based Inverse Dynamic Controller for Throwing Tasks with a Soft Robotic Arm
Diego Bianchi, Michele Gabrio Antonelli, Cecilia Laschi, Angelo Maria Sabatini and Egidio Falotico 424

Curved Surface Inspection by a Climbing Robot: Path Planning Approach for Aircraft Applications
Silya Achat, Julien Marzat and Julien Moras 433

A PLF-CACC Design with Robustness to Communication Delays
Khadir Lakhdar Besseghieur, Abdelkrim Nemra and Fethi Demim 444

SMaNa: Semantic Mapping and Navigation Architecture for Autonomous Robots
Quentin Serdel, Julien Marzat and Julien Moras 453

Design and Control of a Novel High Payload Light Arm for Heavy Aerial Manipulation Tasks
Michele Marolla, Jonathan Cacace and Vincenzo Lippiello 465

Learning Based Interpretable End-to-End Control Using Camera Images
Sandesh Athni Hiremath, Praveen Kumar Gummadi, Argtim Tika, Petrit Rama and Naim Bajcinca 474

Position/Velocity Aided Leveling Loop: Continuous-Discrete Time State Multiplicative-Noise Filter Case
Irina Avital, Isaac Yaesh and Adrian-Mihail Stoica 485

Learning How to Use a Supernumerary Thumb
Ali Seçkin Kaplan, Emre Akın Ödemiş, Emre Doğan, Mehmet Orhun Yıldırım, Youness Lahdili, Amr Okasha and Kutluk Bilge Arıkan 489

Thorough Analysis and Reasoning of Environmental Factors on End-to-End Driving in Pedestrian Zones
Qazi Hamza Jan, Arshil Ali Khan and Karsten Berns 495

High-Velocity Walk-Through Programming for Industrial Applications: A Safety-Oriented Approach
Simone di Napoli, Mattia Bertuletti, Mattia Gambazza, Matteo Ragaglia, Cesare Fantuzzi and Federica Ferraguti 503

2D LiDAR-Based Human Pose Tracking for a Mobile Robot
Zhenyu Gao, Ze Wang, Ludovic Saint-Bauzel and Faïz Ben Amar 511

From Point Cloud Perception Toward People Detection
Assia Belbachir, Antonio M. Ortiz, Atle Aalerud and Ahmed Nabil Belbachir 520

SHORT PAPERS

Smooth Sliding Mode Control Based Technique of an Autonomous Underwater Vehicle Based Localization Using Obstacle Avoidance Strategy
Fethi Demim, Abdenebi Rouigueb, Hadjira Belaidi, Ali Zakaria Messaoui, Khadir Lakhdar Bensseghieur, Ahmed Allam, Mohamed Akram Benatia, Abdelmadjid Nouri and Abdelkrim Nemra 529

Advanced Trajectory Planning and 3D Waypoints Navigation of Unmanned Underwater Vehicles Based Fuzzy Logic Control with LOS Guidance Technique
Fethi Demim, Hadjira Belaidi, Abdenebi Rouigueb, Ali Zakaria Messaoui, Kahina Louadj, Sofian Saghour, Mohamed Akram Benatia, Mohamed Chergui, Abdelkrim Nemra, Ahmed Allam and Elhaouari Kobzili 538

RoboToy Demoulding: Robotic Demoulding System for Toy Manufacturing Industry
Daniel Sánchez-Martínez, Carlos A. Jara and Francisco Gomez-Donoso 546

Design and Control of Wearable Ankle Robotic Device
Ali Zakaria Messaoui, Mohamed Amine Alouane, Mohamed Guiatni, Omar Mechali, Sbargoud Fazia, Zerdani Serine and Belimene Cheikh Elmokhtar 554

Real Time Orbital Object Recognition for Optical Space Surveillance Applications
Radu Danescu, Attila Fuzes, Razvan Itu and Vlad Turcu 562

TEAM: A Parameter-Free Algorithm to Teach Collaborative Robots Motions from User Demonstrations
Lorenzo Panchetti, Jianhao Zheng, Mohamed Bouri and Malcolm Mielle 570

Driver Attention Estimation Based on Temporal Sequence Classification of Distracting Contexts
Raluca Didona Brehar, George Coblişan, Attila Füzes and Radu Dănescu 578

Evaluating Deep Learning Assisted Automated Aquaculture Net Pens Inspection Using ROV
Waseem Akram, Muhayyuddin Ahmed, Lakmal Seneviratne and Irfan Hussain 586

Single Source of Truth: Integrated Process Control and Data Acquisition System for the Development of Resistance Welding of CFRP Parts
Michael Vistein, Monika Mayer, Manuel Endraß and Frederic Fischer 592

On-Board Estimation of Vehicle Speed and the Need of Braking Using Convolutional Neural Networks 600
Razvan Itu and Radu Danescu

Experimental Validation of the Non-Orthogonal Serret-Frenet Parametrization Applied to the Path Following Task 608
Filip Dyba

Dual-Arm Compliance Control with Robust Force Decomposition 616
William Freidank, Konrad Ahlin and Stephen Balakirsky

Robust Single Object Tracking and Following by Fusion Strategy 624
Alejandro Olivas, Miguel Ángel Muñoz-Bañón, Edison Velasco and Fernando Torres

Recognition and Position Estimation of Pears in Complex Orchards Using Stereo Camera and Deep Learning Algorithm 632
Siyu Pan, Ayanori Yorozu, Akihisa Ohya and Tofeal Ahamed

Sensorless Reduction of Cane Oscillations Aimed at Improving Robotic Grapevine Winter Pruning 640
Andrea Fimiani, Pierluigi Arpenti, Matteo Gatti and Fabio Ruggiero

Simultaneous Planning of the Path and Supports of a Walking Robot 648
Paula Mollá-Santamaría, Adrián Peidró, Arturo Gil, Óscar Reinoso and Luis Payá

A Linear Regression Based-Approach to Collective Gas Source Localization 657
Ronnier Frates Rohrich, Luis Felipe Messias, Jose Lima and Andre Schneider de Oliveira

Zeroth-Order Optimization Attacks on Deep Reinforcement Learning-Based Lane Changing Algorithms for Autonomous Vehicles 665
Dayu Zhang, Nasser Lashgarian Azad, Sebastian Fischmeister and Stefan Marksteiner

An Efficient Resilient MPC Scheme via Constraint Tightening Against Cyberattacks: Application to Vehicle Cruise Control 674
Milad Farsi, Shuhao Bian, Nasser L. Azad, Xiaobing Shi and Andrew Walenstein

Muscle-Like Soft Actuation for Motor-Less Robotic Exoskeletons 683
Julian D. Colorado, John E. Bermeo, Fredy A. Cuellar, Catalina Alvarado-Rojas, Diego Mendez, Angela M. Iragorri and Ivan F. Mondragon

Development of Cart with Providing Constant Steerability Regardless of Loading Weight or Position: 3rd Report on Evaluation of a Steering Assist System on Translational Movement 689
Shunya Aoki, Sho Yokota, Akihiro Matsumoto, Daisuke Chugo, Satoshi Muramatsu, Katsuhiko Inagaki and Hiroshi Hashimoto

Modelling of a 6DoF Robot with Integration of a Controller Structure for Investigating Trajectories and Kinematic Parameters 697
Armin Schleinitz, Chris Schöberlein, Andre Sewohl, Holger Schlegel and Martin Dix

Soft Robotic Tongue Mimicking English Pronunciation Movements 2 Report: Fabrication and Experimental Evaluation 704
Evan Krisdityawan, Sho Yokota, Akihiro Matsumoto, Daisuke Chugo, Satoshi Muramatsu and Hiroshi Hashimoto

Low-Cost Synchronization Techniques for KUKA Robots and External Axes in Low-Dynamic Processes 711
Patrick Kaufmann, Holger Weber and Michael Vistein

A Decision-Making Architecture for Human-Robot Collaboration: Model Transferability
Mehdi Sobhani, Jim Smith, Anthony Pipe and Angelika Peer 719

Evaluation of Low-Cost 3D Scanner Hardware for Clothing Industry
Michael Danner, Elena Alida Brake, Christian Decker, Matthias Rätsch, Yordan Kyosev and Katerina Rose 727

Shape Transformation with CycleGAN Using an Automobile as an Example
Akira Nakajima and Hiroyuki Kobayashi 736

Development of Walking Assistance Orthosis by Inducing Trunk Rotation Using Leg Movement: 1st Report on Prototype and Feasibility Experiment
Harutaka Ooki, Sho Yokota, Akihiro Matumoto, Daisuke Chugo, Satoshi Muramatsu and Hiroshi Hashimoto 740

A Study on Gathering Staircase Information for Active Staircase Entry of Wheelchair Stair Climbing Assistive Devices
Su-Hong Eom, Jeon-Min Kang, Ga-Young Kim and Eung-Hyuk Lee 747

Longitudinal Motion Control of Underactuated Cruising AUVs for Acoustic Bottom Survey
Kangsoo Kim 754

LQR Combined with Fuzzy Control for 2-DOF Planar Robot Trajectories
A. Hernandez-Pineda, I. Bezerra-Viana, M. Marques-Simoes and F. Carvalho Bezerra 763

Sustainability in Robotic Process Automation: Proposing a Universal Implementation Model
Christian Daase, Anuraag Pandey, Daniel Staegemann and Klaus Turowski 770

AUTHOR INDEX 781

Simultaneous Planning of the Path and Supports of a Walking Robot

Paula Mollá-Santamaría[1][a], Adrián Peidró[1][b], Arturo Gil[1][c], Óscar Reinoso[1,2][d] and Luis Payá[1][e]
[1]Instituto de Investigación en Ingeniería de Elche (I3E), Universidad Miguel Hernández de Elche,
Avda. de la Universidad s/n, Edificio Innova, 03202 Elche, Alicante, Spain
[2]ValgrAI: Valencian Graduate School and Research Network of Artificial Intelligence,
Camí de Vera s/n, Edificio 3Q, 46022 Valencia, Spain
{pmolla, apeidro}@umh.es

Keywords: Path Planning, Support Planning, Stability, Non-Coplanar Contacts, Walking Robot.

Abstract: In this paper we study the simultaneous planning of the path and leg supports of an eight-legged robot on uneven terrain. We use the A-star algorithm (A*), which searches for the shortest path between two points. First, the terrain is modelled with a triangular mesh and the triangles are subdivided to take the centroids of these triangles as the search space of the A*. Secondly, with respect to the original A*, the stability of the robot at each centroid is considered, so that the cost at a centroid is penalised if the robot is unstable (i.e., the robot slips and/or tips over), or the cost is zero if it is stable. The stability at each contact point is determined by calculating that the ground reaction at that point is contained in a linear approximation of the friction cone. Finally, the path, the contact points of each leg, as well as the robot's posture at each position are obtained.

1 INTRODUCTION

This paper presents a solution for the path planning of an eight-legged modular robot in rough natural terrains consisting of different slopes. We determine the sequence of positions and orientations that the robot must visit in order to move from an initial point to a final point of the terrain, including the supports or footholds where the robot must place all feet for each position of the path, to guarantee stability, i.e., to prevent slipping and tipping over.

For legged robots moving on horizontal planes with sufficient friction to prevent slippage, one of the most extended stability tests is based on the Zero Moment Point (ZMP) (Vukobratović and Borovac, 2004), which is the point respect to which contact moments have no horizontal components. If the ZMP belongs to the convex hull of the support points, the robot will not tip over.

For robots with legs supported on different planes, or when the ground cannot offer sufficient friction to neglect slippage, the ZMP test is insufficient and the Contact Wrench Cone (CWC) (Hirukawa et al., 2006) should be studied instead. The CWC is based on the idea that, for each point of contact of the robot with the ground, there is a reaction force from the ground that should be inside a friction cone whose axis is normal to the ground and whose aperture depends on the coefficient of friction. For computational efficiency, such friction cones are approximated by inscribed pyramids. The vectors $\mathbf{f}_{ij}$ along the lateral edges of these pyramids, together with their moments, constitute a set of 6-dimensional wrenches that, counted for all contact points of the robot, span the 6-dimensional Contact Wrench Cone. If the net wrench acting on the robot due to inertia, gravity and external forces (excluding reactions from the ground) belongs to the CWC, the robot will not tip over or slip.

The CWC has been widely used to plan the dynamically stable locomotion of legged robots, both bipedal humanoids (Dai y Tedrake, 2016; Navaneeth, Sudheer, and Joy, 2022) and quadrupedal (Aceituno-Cabezas et al., 2017). Most papers depart from a precomputed set of footholds along the terrain, at

---

[a] https://orcid.org/0009-0003-5447-0278
[b] https://orcid.org/0000-0002-4565-496X
[c] https://orcid.org/0000-0001-7811-8955
[d] https://orcid.org/0000-0002-1065-8944
[e] https://orcid.org/0000-0002-3045-4316

Mollá-Santamaría, P., Peidró, A., Gil, A., Reinoso, Ó. and Payá, L.
Simultaneous Planning of the Path and Supports of a Walking Robot.
In *Proceedings of the 20th International Conference on Informatics in Control, Automation and Robotics (ICINCO 2023) - Volume 1*, pages 648-656
ISBN: 978-989-758-670-5; ISSN: 2184-2809
Copyright © 2023 by SCITEPRESS – Science and Technology Publications, Lda. Under CC license (CC BY-NC-ND 4.0)

which the robot should support its legs during the trajectory, and then they focus on solving the trajectory of the center of mass to guarantee that gravito-inertial wrenches are in the CWC within some margin, while minimizing centroidal angular momentum. Recent papers such as (Aceituno-Cabezas et al., 2018) or (Jenelten, Grandia, Farshidian, and Hutter, 2022) do not assume a precomputed set of footholds, which are planned at the same time that the global locomotion of the robot, solving mixed-integer convex optimization problems or using graduated optimization techniques. The simultaneous planning of the path of the robot and of the footholds yields more optimal and natural solutions. Other remarkable works that use the CWC are (Orsolino et al., 2018), where the CWC is intersected with a polytope that considers limits on actuation torques, or Ellenberg and Oh (2014), who use the CWC to analyze the stability of humanoids climbing ladders, taking into account limits on the contact wrenches that the environment can provide.

Typically, the stability test based on the CWC is computationally demanding, considering that it requires many operations to first build a polytope that is the convex hull of dozens of 6-dimensional contact wrenches, and then check if the gravito-inertial wrenches acting on the robot belong to this polytope. Some papers have tried to reduce the cost of these operations to check stability while controlling the robot in real time. Li et al. (2022) present a simplified test that approximates the contact polygon by an effective segment, sacrificing accuracy for efficiency. Caro and Kheddar (2016) change checking the 6D polytope for checking if the centroidal acceleration belongs to a 3D volume. Finally, Caron, Pham and Nakamura (2017) project the CWC on a 2D polygon to which the ZMP should belong to guarantee stability, generalizing the notion of ZMP to situations with insufficient friction or non-coplanary contacts.

In this paper, we present a solution for the simultaneous planning of the path and supports of a modular eight-legged robot described in Section 2, which should explore natural terrains consisting of planes with different orientations where slippage cannot be neglected. First, in Section 3, we describe the modeling of the terrain, which is approximated by a triangular mesh. Next, in Section 4, we present the stabilty test, which avoids building the 6-dimensional CWC and instead solves iteratively a quadratic and underdetermined system of equations using the Newton-Raphson method, performing the stability test roughly 10 times faster than by building the CWC. Section 5 proposes our algorithm to simultaneously plan the path and supports of the legged robot, which is based on the A-star (A*) algorithm, but incorporating instability as a penalty to the cost function (among other sub-costs). Then, Section 6 illustrates the developed algorithm by means of examples. These examples demonstrate the feasibility of the paths planned by the proposed algorithm, comparing the results obtained when considering stability or when ignoring it (in which case, the robot would fall down steep inclines). Finally, Section 7 summarizes the conclusions and suggests future lines of research, which will be mainly directed towards speeding up the proposed method, so that it can be used in real time.

2 ROBOT DESCRIPTION

This section describes the modular walking robot whose optimal path is planned in this paper, from an initial to a final position in a rugged natural environment, also determining the contact points on the ground.

The robot presented in Figure 1 consists of two identical modules connected by a spherical or ball joint. The modules have a central body that can move and orient itself in the x, y, and z axes and four legs with three degrees of freedom each (q_1, q_2, q_3) that allow it to move efficiently, where q_1 provides the forward and backward movement of the leg, q_2 allows the raising and lowering of the leg, and q_3 facilitates the bending or stretching of the leg. Each module of the robot has eighteen degrees of freedom, giving it great freedom of movement for moving over rough terrain.

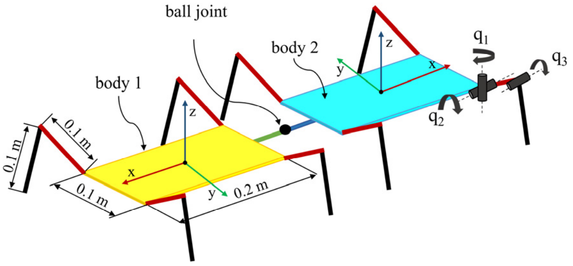

Figure 1: Wireframe representation of the studied modular legged robot.

3 TERRAIN MODELLING AND SUBDIVISION

The planning of the robot's path and the determination of the points of contact with the environment are the objectives of this article. To this purpose, this section describes the modelling and pre-processing of the terrain on which the robot moves, considering that all the robot's feet will be resting on the ground at each position of the planned path.

The modelled terrain consists of several ramps with different inclinations surrounding the environment, requiring the robot to climb three ramps to reach the highest point. It is important to note that the initial terrain is defined by a triangular mesh in STL format. To achieve this, we first used 3D design software, specifically Autodesk Inventor, to create the CAD model of the terrain. Then, we exported the model in STL format, as this format is capable of representing solid objects by approximating their surface with triangles in a graphical manner. In real scenarios, a point cloud of the environment may be obtained using range sensors, and this point cloud may be used as the starting point to model the terrain in a similar way as described in this paper.

To undertake the planning of the robot's path, it is necessary to start with a point cloud to identify the nodes or points that will be part of the optimal path from the initial to the final position. Since the terrain is composed of triangles, the centroids of these triangles are used as search points for the path. In order to obtain a denser mesh of nodes and to achieve a more accurate and realistic planning, a recursive subdivision of the terrain is performed, dividing the triangles into smaller ones. This subdivision process continues until each triangle is circumscribed within a circle of radius less than 0.2 m.

The subdivision method implemented consists in dividing each triangle by connecting the centres of its sides, which generates four new triangles. However, this method requires multiple subdivisions to get the most elongated or flattened triangles to be circumscribed within a circle of radius R, as shown in Figure 2b. In our case, the flattened triangles are in an area of the terrain that the robot will not traverse, therefore, this does not affect the path planning. However, to obtain a more equiaxial subdivision of the triangles which form the terrain, an alternative method could be considered. This procedure would consist in dividing the longest side of the triangle into N segments, using a value of 10 for N, and then joining these segments with the opposite vertex.

Figure 2 below illustrates both the original terrain and the subdivided terrain.

One of the objectives of the article is to identify the location of the robot's footholds on the subdivided terrain. To achieve this, the triangle of the terrain closest to each foot of the robot is found and a projection of the foot onto this triangle is made. This process is repeated for each of the robot's legs.

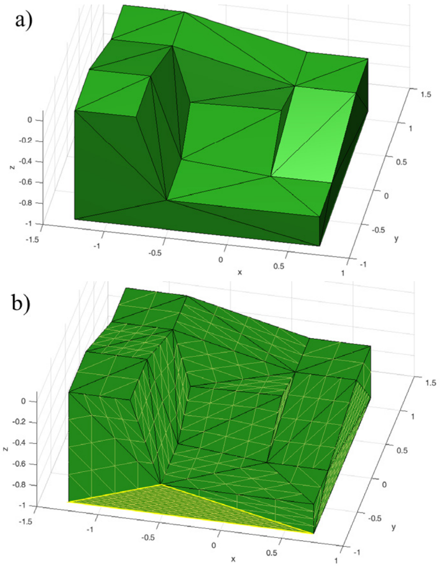

Figure 2: a) Original terrain. b) Subdivided terrain.

Initially, a brute force search was used to find the closest triangle by checking all triangles in the environment. However, this approach proved computationally expensive. To improve the search process, we decide to examine only triangles that are within a short distance of the robot's shoulder. To do this, a k-d tree is created using the centroids of the subdivided triangles that make up the terrain. Through this k-d tree, the centroids that lie within a sphere centred at the shoulder of the leg, with a radius of r*1.5, are determined. In this case, r has a value of 0.2, corresponding to the total length of the robot leg when fully extended.

Once the triangle closest to the foot of each leg has been identified, the projection of each foot on the closest triangle is calculated. This ensures that the robot, in each position, has all its legs correctly supported on the ground, which makes it possible to analyse its stability, as described in the next section.

4 STABILITY ANALYSIS

Stability plays a crucial role in the robot's path planning, since if it moves along an unstable path, it could face tipping or slipping situations, compromising both its safety and accuracy in task execution.

In order to guarantee the stability of the robot, it is essential to carry out an analysis of the support points. The Zero Moment Point (ZMP) is the point at which the reaction forces produced at the robot's contacts with the ground do not generate any moment in the horizontal direction. In planar horizontal grounds with sufficient friction, the ZMP must be within the convex hull of the robot's contact points with the ground for the robot to be in a stable position. However, this analysis becomes more complex for robots with multiple non-coplanar contacts, or when friction is not sufficiently high to neglect slippage. In this context, Hirukawa et al. (2006) proposed a more general stability criterion based on the Contact Wrench Cone (CWC), which addresses this issue by considering the friction constraints between the contact points and the ground.

In this method, the stability of a contact point C_i is evaluated by the contact force $\mathbf{f}_i$, which is the vector sum of the normal reaction along the normal $\mathbf{n}_i$ at the contact point, and the friction force tangent to the ground, $\mathbf{f}_{friction}$. For a contact point to be considered stable, the contact force is required to be within the friction cone, defined as:

$$\|\mathbf{n}_i \times \mathbf{f}_i \times \mathbf{n}_i\|_2 \leq \mu_i(\mathbf{f}_i \cdot \mathbf{n}_i) \tag{1}$$

where μ_i is the coefficient of friction.

In numerous articles, such as (Caron et al. 2017), a linear approximation of the friction cone is used due to its better computational efficiency in terms of computational speed and processing. This approximation consists in approximating the cone by an inner pyramid whose lateral edges are denoted by $\mathbf{f}_{ij}$, as shown in Figure 3. To ensure the stability of the robot, condition (2) must be fulfilled, which involves the $\mathbf{f}_{ij}$ vectors and their moments, considering the position of C_i in relation to the global coordinate system, defined as $\mathbf{p}_{Ci}$.

$$\begin{bmatrix} \mathbf{f} \\ \boldsymbol{\tau}_O \end{bmatrix} = \sum_{ij} \lambda_{ij} \begin{bmatrix} \mathbf{f}_{ij} \\ \mathbf{p}_{C_i} \times \mathbf{f}_{ij} \end{bmatrix} \quad \lambda_{ij} \geq 0 \tag{2}$$

where the subscript i iterates over the contact points ($i = 1 \ldots 8$ for the legged robot described in Section 2) and j iterates over the edges used in the approximation of the friction cones by pyramids.

Equation (2) establishes that the resultant of the external forces $\mathbf{f}$ and moments $\boldsymbol{\tau}_O$ (due to gravity, inertia, etc.) that could cause the robot to tip over or slip, must be a linear combination of the vectors $\mathbf{f}_{ij}$ and their moments, multiplied by non-negative coefficients λ_{ij}. This ensures the stability of the robot by guaranteeing that the $\mathbf{f}_i$ reactions are within the friction pyramid. In this article, 10 $\mathbf{f}_{ij}$ vectors have been used to approximate the friction cone at each contact point, although for simplicity only 6 edges are represented in Figure 3.

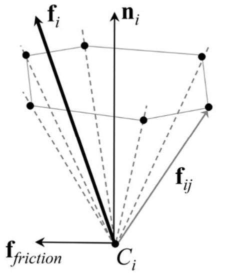

Figure 3: Stable Contact C_i.

Typically, the stability test consists in building the 6-dimensional CWC cone represented by the right-hand side of (2), and checking if the left-hand side of (2), i.e., the 6-dimensional vector $[\mathbf{f} ; \boldsymbol{\tau}_O]$, belongs to this CWC, in which case the robot is stable. However, building the CWC is a costly operation, and in this paper we will use a simpler method to check if (2) admits a solution consisting of non-negative λ_{ij} for a given wrench $[\mathbf{f} ; \boldsymbol{\tau}_O]$, as explained next.

The stability test employed in this paper begins by transforming the inequality constraints of (2) into equivalent equalities, by defining a new auxiliary variable t_{ij} for each λ_{ij}, and then replacing each inequality $\lambda_{ij} \geq 0$ by its equivalent quadratic equation:

$$\lambda_{ij} = t_{ij}^2 \tag{3}$$

After this, (2) becomes a quadratic system of six equations with many more than six unknowns λ_{ij} and t_{ij} (e.g., if each friction cone is approximated by a 10-sided pyramid, and having eight contact points, we have 80 × 2 unknowns λ_{ij} and t_{ij}). This underdetermined system is solved by the iterative Newton-Raphson method, using the pseudoinverse of the Jacobian matrix that gives the least norm solution.

If we make several attempts (e.g., 10) to obtain a converging solution using the Newton-Raphson method as explained above, where each attempt starts from a different random value of λ_{ij} and t_{ij}, and all attempts fail to converge after a reasonable number of iterations, then we conclude that the robot is unstable, as it is impossible to find non-negative λ_{ij} that satisfy (2) for the given left-hand side $[\mathbf{f} ; \boldsymbol{\tau}_O]$. Otherwise, if at least one attempt converges to a solution, then we conclude that the robot is stable.

By running several examples where stability was tested using the described Newton-Raphson method or the typical method that requires building the 6-dimensional CWC, we checked that both methods always gave the same verdict of stability, but the Newton-Raphson method performed roughly 10 times faster, and it was easier to implement. This higher speed is advantageous if the stability test must be repeatedly performed many times, as it will be required in the path-planning algorithm described in the next Section. Therefore, in the following, we will test stability using the Newton-Raphson method described above.

5 PLANNING THE PATH AND CONTACT POINTS

The aim of this paper is to perform simultaneous planning of the path and locations of footholds of the multi-legged robot introduced in Section 2. To achieve this, we implement the A-star search algorithm (A*), which searches for the path with the lowest cost from an initial position to a final position. We use the A* algorithm to find a sequence of waypoints of the terrain at which the robot can be positioned and oriented stably without suffering tipping over or slipping, with all its eight feet supported on the terrain. We do not solve, however, the sequence of movements that the robot needs to execute to move from one waypoint to the next one, i.e., lifting and swinging each leg to move the robot while other legs rest on the terrain. This latter problem is left for future work.

In our approach, we start from a terrain subdivided into triangles, whose known centroids form a grid of points that serves as the search space for the algorithm. Using these points, a k-d tree is constructed and used at the beginning of the algorithm to find the initial and final nodes closest to the desired initial and final positions provided by the user or high-level path planner. In addition, while the algorithm executes the steps described later, the same k-d tree is also used to find the *n* nearest neighbour nodes to the current node, where in this example, *n* is equal to 10. The use of k-d trees allows us to make these searches more efficiently compared to an exhaustive brute-force search.

In this paper, in order to obtain the optimal route, the A* algorithm is used to carry out an exploration along all the centroids (nodes) of the triangles representing the terrain. A variant of the conventional A* algorithm is used, where the distances or costs associated with each node are modified, taking into consideration both the stability of the robot and the similarity between the configurations or postures adopted by the robot between neighbour nodes. The algorithm implemented in this article can be summarised in the following steps:

1) The algorithm explores all the nodes that are part of the terrain map, starting with the initial node and prioritising the search among those nodes with the lowest cost f (the definition of cost f will be provided later).
2) After that, the 10 nearest $neighbour$ nodes to the current node are determined (initially, the current node is the initial node).
3) The costs f and g are obtained for each of the neighbouring nodes that have not been previously evaluated or explored.

$$\begin{gathered} g\,(neighbour) = g(current) + d + q + e \\ f(neighbour) = g(neighbour) + h \end{gathered} \tag{4}$$

where:

- $g(x)$ represents the real cost of reaching node “x” from the initial node.

- $f(neighbour)$ is an estimate of the total cost of going to the destination node from the initial node, passing through the $neighbour$ node. This cost is calculated using a distance heuristic h that must not overestimate the actual distance. In this case, for simplicity, the straight-line distance between the $neighbour$ and the destination is used as the heuristic h.

- d is the actual distance between the $current$ node and the $neighbour$.

- q represents the difference between the configurations adopted by the robot when resting at the $current$ node and at the $neighbour$ node. The difference in positions and orientations of the robot's modules, as well as the joint angles rotated by its legs, between the posture at the $current$ node and at the $neighbour$ node is considered. The objective is to minimise q to try to achieve continuity in the postures adopted by the robot along the various nodes it travels during the path.

- e is a penalty for lack of stability. By applying the method described in Section 4, the stability of the robot when placed on the $neighbour$ node is evaluated. In situations where instability is identified, a significantly high value is assigned to e as a penalty, so that the A* algorithm will discard that node as part of the potential path to the destination node. In contrast, if the robot is stable, e is set to 0.

It is important to consider that q and e are dependent on the orientation adopted by the robot when it is positioned over the $neighbour$ node. To tackle this, four orientations separated by 45 degrees are explored, as it will be explained later. The orientation that yields the lowest value for the sum of q and e is selected.

The next subsection details the process of "building" the robot's posture as it is placed over each

$neighbour$ node. This is done in order to evaluate all the previously mentioned costs.

5.1 Building the Posture of the Robot at Each Node

To calculate the different costs involved in (4), the robot must be placed at a given position with all eight feet resting on the ground. This requires defining the footholds for all feet, the position and orientation of the central body of each of the two modules that integrate the robot, and the joint angles of every leg. This subsection will describe the calculations that allow us to define a reasonable and feasible posture of the robot when placed over each node visited by the A* algorithm. This feasible posture will be obtained by first building a tentative posture, and later refining it using Newton-Raphson iterations, to guarantee that all feet of the robot rest on the ground.

First, the spherical or ball joint connecting the two robot modules, called *C*, is placed at a distance *a* from the node or centroid of the triangle being evaluated, along the direction normal **n** to the triangle. Then, a principal axis called **ep** is defined, which is taken as any vector perpendicular to the normal **n**. This vector **ep** represents the main axis of the robot, i.e., the axis along which both bodies depicted in Figure 1 would be aligned if the robot adopted a posture so symmetric and “straight” as that shown in Figure 1. Evidently, since the terrain over which the robot moves is not flat, the final posture adopted by the robot at each node (this final posture will be constructed in the following paragraphs of this section) will not be so symmetric and straight as in Figure 1, but it will still be somewhat oriented in the direction of **ep**.

After aligning the bodies with the principal axis **ep**, the coordinate frames of each body, which define the orientation of each body, are calculated as shown in Figure 4. To this end, the bodies are arranged perpendicular to the normal $\mathbf{n}_{bi}$ of the triangle located directly below the centre of each body *i*. The normal of the body corresponds to the z-axis, while the x-axis is defined as the normalized projection of the principal axis **ep** on the plane of the body. Finally, the y-axis is obtained by the cross product of the z-axis and the x-axis.

In addition, the centres of the bodies are determined as the intersection between each of the x-axes of the bodies (regarded as infinite lines passing through the spherical joint *C*) and a sphere of radius *R*, centred at *C*, as illustrated in Figure 5.

The intersection points between the sphere and the x-axes gives:

$$\begin{aligned} x_{bi} &= x_o + R \cdot x_{1,bi} \\ y_{bi} &= y_o + R \cdot x_{2,bi} \\ z_{bi} &= z_o + R \cdot x_{3,bi} \end{aligned} \qquad (5)$$

where $R = l + L_c/2$ is the sum of the length l of the little segment that joins each body to the spherical joint *C*, and L_C is the length of each body along its x-axis. On the other hand, x_o, y_o and z_o correspond to position of joint *C*, while the coordinates x_{bi}, y_{bi}, z_{bi} represent the centre of body *i*. $x_{1,bi}$, $x_{2,bi}$, and $x_{3,bi}$ are the components of the unit vector of the x-axis of each body *i*.

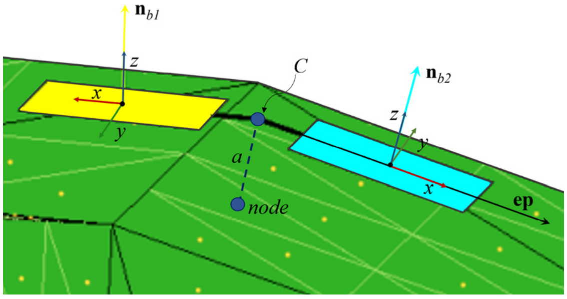

Figure 4: Central bodies of the robot without legs in the ***ep*** direction.

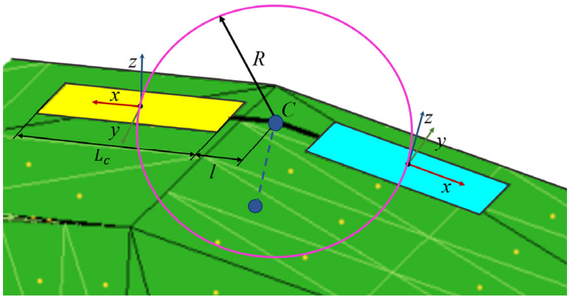

Figure 5: Intersection of the sphere centred at *C* with the x-axis of each body.

After defining the position and orientation of each body, the four legs are added to each body. Initially, these legs are added forming exactly a right angle with respect to the body, similar to the legs of the yellow body shown in Figure 6. Note that, if the terrain under the bodies of the robot is not flat for the node that is being evaluated, in general, some of the feet may not be in contact with the terrain after placing the legs at right angles as indicated here. Indeed, if the terrain below the body is concave, some legs may penetrate under the terrain, and if the terrain is convex, some feet may be in the air above the terrain, not touching it. However, this is not a problem because the final posture of the robot will be corrected using the Newton-Raphson method as explained later, so that it correctly rests on the terrain, with all feet in contact with the ground.

The penultimate operation to build the tentative posture of the robot when placed over each node consists in finding the points of contact where each foot should be placed (as said in the previous paragraph, some feet may be under the terrain if it is concave, or over it if it is convex). This is done by finding the projection of each foot on the closest triangle of the terrain, as explained at the end of Section 3. These projections are the footholds where each foot should be placed.

Finally, the last operation to complete the calculation of the posture of the robot when placed over each node of the terrain, consists in defining a set of loop-closure equations that represent the following constraints: each foot of the robot should be placed at the corresponding closest foothold, and both bodies should be joined by the spherical joint *C*. These constraints define a system of nonlinear equations whose unknows are the position and orientation coordinates of each body, as well as the joint angles (q_1, q_2, q_3) of each leg (recall these joint angles in Figure 1). This nonlinear system is solved using the Newton-Raphson method, starting the iterations from the tentative posture built by following all the operations described in this subsection 5.1. The result of these iterations is a realistic and feasible posture of the robot with both bodies joined at *C* and all feet resting on the ground, as illustrated in Figure 6. This feasible posture will be similar to the tentative posture which is used as the seed of the Newton-Raphson iterations.

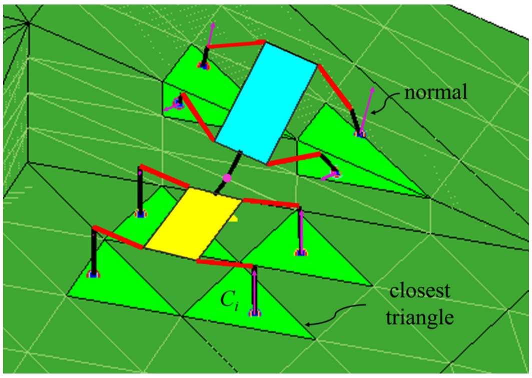

Figure 6: The robot with all its legs resting on the ground.

Once the robot adopts a feasible posture on the ground, its stability is tested using the method described in Section 4, obtaining the sub-cost *e* used in (4). The difference between this posture at the current node and that at its neighbour is also calculated, to obtain the value of the sub-cost *q* used also in (4). All calculations described in this subsection 5.1 are repeated three more times, but each time rotating the main axis ***ep*** about **n** by 45º with respect to the previous time, so that different postures of the robot are tested to roughly cover all possible orientations about axis **n**, finally retaining the posture that gives a smaller value of $e + q$. This is added to the sub-costs d and h of (4), to complete the calculation of the cost at each node, making it possible for the A* algorithm to determine the shortest route to move from a starting point to an end point.

After executing the A* algorithm, it returns the centroids of the subdivided triangles of the terrain that form part of the optimal path, the information of the posture of the robot at each node of the optimal path (orientations and positions of the central bodies and joint angles of the legs), and the support points for all legs, at each node. This will be illustrated with some examples in the next section.

6 RESULTS

The evaluation of the effectiveness of the algorithm A* for calculating the path and the determination of the robot positions and contact points has been carried out in this Section 6. For this purpose, two examples have been studied, which are significant and representative for the method because they require the robot to climb or descend an irregular terrain with several slopes. For each example, an initial and a final position have been defined, and the resulting paths have been compared, considering or ignoring the influence of the stability of the robot in each position until the target position is reached. In the study, a friction coefficient of 0.4 has been considered.

In the first study, the robot must ascend the first ramp and reach an intermediate position on the second ramp (P_A [0, 0.75, -0.2]), starting from an initial position in the lowest part of the terrain (P_O [0, 0, -0.5]). To evaluate the optimal path from P_O to P_A without taking stability into account, Figure 7a, the A* algorithm takes 135 seconds to find the path (this algorithm was implemented in Matlab 2015a on Windows, and it was run on an Intel(R) Core(TM) i7-8750H CPU @ 2.20 GHz processor with 16 GB RAM). The red dots in Figure 7 represent the centroids of the triangles forming part of the optimal path where the projection of the centre of the robot's bodies, C, would be placed and the robot's position would be constructed as explained in section 5.1. The path obtained (Figure 7a) shows how the robot goes straight up to P_A on the steep part of the second ramp, where we should expect that the robot would lose stability and tip over or slip, as the next simulation confirms.

On the other hand, when stability is taken into account for optimal path finding, Figure 7b, the robot goes up the ramps that have an inclination that does not compromise its stability, even though this implies a longer path. In that case, the algorithm requires a response time of 544 seconds to find the optimal path. However, this path ensures that the robot is stable throughout the entire route, avoiding possible tipping or slipping problems.

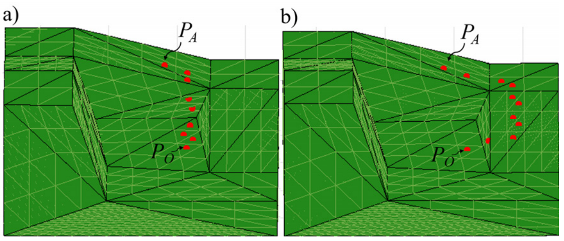

Figure 7: a) Optimal path of the robot from P_O to P_A without stability (red dots). b) With stability.

Furthermore, the A* algorithm simultaneously provides the robot's positions and the contact points at each node of the obtained path. Figure 8 shows some of the robot positions along the path shown in Figure 7b, considering the stability and orientation of the robot.

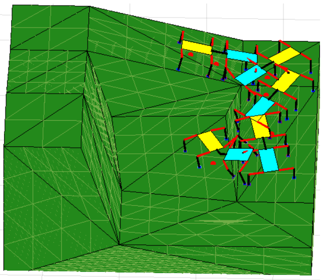

Figure 8: Positions and contacts of the robot in the path to P_A.

In the second example studied, the optimal path is calculated for the robot to descend from the highest point of the terrain P_B [-1, -0.4, 0.2] to the point P_O, Figure 9. Note that this example requires the robot to traverse most of the terrain and, therefore, it includes other example paths in which the robot may need to travel between intermediate points of the terrain.

On the one hand, similar to the previous example, the robot path is calculated using the A* algorithm without taking stability into account, Figure 9a. In this case, the algorithm takes 247 seconds to determine the path with the lowest cost, which is the one that goes straight to P_O down the ramp with a steep slope where the robot would evidently not be stable and would tip over.

On the other hand, when considering the stability of the robot in the path calculation (Figure 9b), the response time of the algorithm increases significantly, reaching approximately 1 hour and 9 minutes. This is because the robot must avoid going straight down the steep ramp to maintain its stability. Instead, it needs to travel a longer path, involving more nodes, to reach the end point safely.

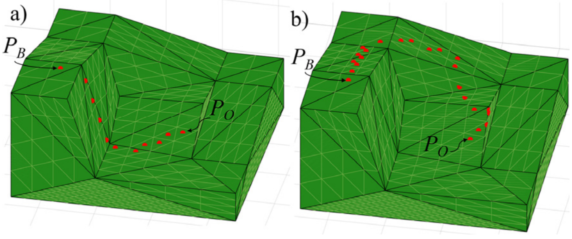

Figure 9: a) Optimal path of the robot from P_B to P_O without stability (red dots). b) With stability.

Figure 10 shows some of the robot positions (postures and contact points) going through the optimal robot path obtained by algorithm A* to reach P_O from the position P_B, ignoring robot stability, Figure 10a, and considering stability, Figure 10b.

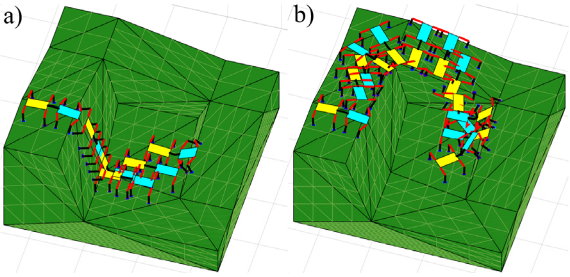

Figure 10: a) Positions and contacts of the robot in the path to P_O without stability. b) With stability.

The algorithm was run again to plan a path from P_O to P_B, i.e. to climb the terrain instead of descend it, and it took 1hour and 42 minutes, which is about 30 minutes more than the time taken to compute the descending path. More simulations were run between initial and final points near P_O and P_B, and in all of them we observed that the time to find an ascending path was slightly higher than to find a descending one. This can be explained by the fact that, when starting up, many of the nodes of the terrain belong to steep slopes at which the robot is unstable, so the search is more directed than when starting down, where the nodes yield stable postures and there are more options to explore.

7 CONCLUSIONS

This paper describes a method for path planning of multi-legged robots in irregular environments. To tackle this challenge, a method has been proposed that starts with the creation of a triangular mesh to define the contact points of the legs and establish a mesh of nodes for path planning. After this, the A* algorithm has been used to find the optimal path from an initial position to the target position, ensuring that the robot maintains stability along the path and adopts realistic and coherent configurations.

This method has also made it possible to identify, at each point in the path, the robot's contact points and postures, providing a representation of its positions in the environment.

However, considering that the robot will need to plan the next path while it executes the current one, it will be crucial to improve the search times of the current algorithm. In this context, a promising strategy to increase efficiency is to explore the use of Rapidly Exploring Random Trees (RRT) instead of the A* algorithm. Although the A* algorithm is capable of finding the absolute optimal path, its high computational cost limits it in applications requiring real-time computations. On the other hand, the RRT algorithm offers faster search times, although the solutions found may be sub-optimal compared to the exhaustive approach of the A* algorithm.

As another future line of research, it will be necessary to address the planning of the movements between successive postures, i.e.: for every two neighbouring postures of the optimal path obtained by the algorithm, it will be necessary to determine a sequence of movements to transform one posture into another (sequence of raising and swinging legs, etc.), while keeping stability.

ACKNOWLEDGEMENTS

This work is part of the INVESTIGO 2022 Programme (file number: INVEST/2022/432) funded by the Valencian Conselleria d'Innovació, Universitats, Investigació i Societat Digital, and by the European Union (Next Generation EU); and of the CIGE/2021/177 project, funded by the Valencian Conselleria d'Innovació, Universitats, Ciència i Societat Digital.

REFERENCES

Aceituno-Cabezas, B., Dai, H., Cappelletto, J., Grieco, J. C., Fernández-López, G. (2017). A mixed-integer convex optimization framework for robust multilegged robot locomotion planning over challenging terrain. En: 2017 *IEEE/RSJ International Conference on Intelligent Robots and Systems*, pp. 4467–4472.

Aceituno-Cabezas, B., Mastalli, C., Dai, H., Focchi, M., Radulescu, A., Caldwell, D. G., Cappelletto, J., Grieco, J. C., Fernández-López, G., Semini, C. (2018). Simultaneous contact, gait, and motion planning for robust multilegged locomotion via mixed-integer convex optimization. *IEEE Robotics and Automation Letters* 3(3), 2531–2538.

Caron, S., Kheddar, A. (2016). Multi-contact walking pattern generation based on model preview control of 3D CoM accelerations. In *2016 IEEE-RAS 16th International Conference on Humanoid Robots*, pp. 550–557.

Caron, S., Pham, Q. C., Nakamura, Y. (2017). ZMP support areas for multicontact mobility under frictional constraints. *IEEE Transactions on Robotics* 33(1),67–80.

Dai, H., Tedrake, R. (2016). Planning robust walking motion on uneven terrain via convex optimization. En: 2016 *IEEE-RAS 16th International Conference on Humanoid Robots*, pp. 579–586.

Ellenberg, R. W., Oh, P. Y. (2014). Contact wrench space stability estimation for humanoid robots. In *2014 IEEE International Conference on Technologies for Practical Robot Applications*, pp. 1–6.

Hirukawa, H., Hattori, S., Harada, K., Kajita, S., Kaneko, K., Kanehiro, F., Fujiwara, K., Morisawa, M. (2006). A universal stability criterion of the foot contact of legged robots-Adios ZMP. En: 2006 *IEEE International Conference on Robotics and Automation*, pp. 1976–1983.

Jenelten, F., Grandia, R., Farshidian, F., Hutter, M. (2022). TAMOLS: Terrain-aware motion optimization for legged systems. *IEEE Transactions on Robotics* 38(6), 3395–3413.

Li, S., Chen, H., Zhang, W., & Wensing, P. M., (2022). A geometric sufficient condition for contact wrench feasibility. *IEEE Robotics and Automation Letters* 7(4), 12411–12418.

Navaneeth, M. G., Sudheer, A. P., Joy, M. L. (2022). Contact wrench cone-based stable gait generation and contact slip estimation of a 12-DOF biped robot. *Arabian Journal for Science and Engineering* 47, 15947–15971.

Orsolino, R., Focchi, M., Mastalli, C., Dai, H., Caldwell, D. G., Semini, C. (2018). Application of wrench-based feasibility analysis to the online trajectory optimization of legged robots. *IEEE Robotics and Automation Letters 3*(4), 3363–3370.

Vukobratović, M., Borovac, B. (2004). Zero-moment point—thirty five years of its life. *International Journal of Humanoid Robotics 1*(1), 157–173.